Available online at www.sciencedirect.com
ScienceDirect
Electrochimica Acta 51 (2006) 6406–6411
ELECTROCHIMICA Acta
www.elsevier.com/locate/electacta

Enhanced high-potential and elevated-temperature cycling stability of $LiMn_2O_4$ cathode by TiO_2 modification for Li-ion battery

Lihong Yu, Xinping Qiu *, Jingyu Xi, Wentao Zhu, Liquan Chen

Key Lab of Organic Optoelectronics and Molecular Engineering, Department of Chemistry, Tsinghua University, Beijing 100084, China

Received 16 February 2006; received in revised form 5 April 2006; accepted 13 April 2006
Available online 9 June 2006

Abstract

The surface of spinel $LiMn_2O_4$ was modified with TiO_2 by a simple sol–gel method to improve its electrochemical performance at elevated temperatures and higher working potentials. Compared with pristine $LiMn_2O_4$, surface-modification improved the cycling stability of the material. The capacity retention of TiO_2-modified $LiMn_2O_4$ was more than 85% after 60 cycles at high potential cycles between 3.0 and 4.8 V at room temperature and near to 90% after 30 cycles at elevated temperature of 55 °C at 1*C* charge–discharge rate. SEM studies shows that the surface morphology of TiO_2-modified $LiMn_2O_4$ was different from that of pristine $LiMn_2O_4$. Powder X-ray diffraction indicated that spinel was the only detected phase in TiO_2-modified $LiMn_2O_4$. Introduction of Ti into $LiMn_2O_4$ changed the electronic structures of the particle surface. Therefore a surface solid compound of $LiTi_xMn_{2-x}O_4$ may be formed on $LiMn_2O_4$. The improved electrochemical performance of surface-modified $LiMn_2O_4$ was attributed to the improved stability of crystalline structure and the higher Li^+ conductivity.

Keywords: $LiMn_2O_4$; TiO_2 modification; High-potential stability; Elevated-temperature stability; Differential capacity–potential

1. Introduction

Over the past 20 years, the spinel $LiMn_2O_4$ has been widely studied for the replacement of $LiCoO_2$ as a cathode material in the lithium ion batteries due to its low cost and high safety [1–3]. Unfortunately, the $LiMn_2O_4$ suffers capacity fading during cycling and the fade is severe especially at elevated temperatures above 55 °C [4]. The structure instability, the decomposition of electrolyte, the dissolution of manganese ions, Jahn–Teller distortion, etc. [5–8] were regarded as main reasons for the capacity fade. Up to now, many efforts, such as doping cations [9], optimizing synthesis condition [10], changing synthesis approaches [11–13], treating the surface of the $LiMn_2O_4$ [14], etc., were devoted to improve the cycle performance. Titanium dioxide (TiO_2) has channels which may be used for storage of little cations, such as H^+ and Li^+ [15] and the lithium insertion/extraction to TiO_2 process has also been observed [16]. Thus, we may believe that TiO_2 is a good material for the lithium-ion batteries which allows lithium-ion insertion/extraction and meanwhile has no serious reactions with electrolyte.

To the best of our knowledge, the sol–gel TiO_2-modified $LiMn_2O_4$ has never been reported yet. The purpose of the present work is a first investigation on the improved electrochemical properties of the TiO_2-modified $LiMn_2O_4$ electrode material. Furthermore, this method has been proved a likely promising treatment of the sample $LiMn_2O_4$.

2. Experimental

The pristine $LiMn_2O_4$ powders are obtained from Guangdong HONGSEN Group Co., Ltd. Tetrabutyl titanate was first dissolved in the ethanol (solution 1). At the same time, the ethanol, distilled water and acetic acid glacial were mixed in another container (solution 2). Then solution 1 was added dropwise to the continuously stirred solution 2. The mixture was continuously stirred for 3 h at room temperature after the dropwise addition and by this means the Ti-sol was obtained. Then we added pristine $LiMn_2O_4$ powders into this Ti-sol causing the $LiMn_2O_4$ coated by the Ti-sol with the amount of TiO_2 corresponding to 4 wt% of the $LiMn_2O_4$. The coated $LiMn_2O_4$ mixture was stirred for 12 h and then dried at 95 °C. Finally the

* Corresponding author. Tel.: +86 10 62794234; fax: +: 86 10 62794234.
E-mail address: qiuxp@mail.tsinghua.edu.cn (X. Qiu).

0013-4686/$ – see front matter © 2006 Elsevier Ltd. All rights reserved.
doi:10.1016/j.electacta.2006.04.054

coated $LiMn_2O_4$ powders were calcined at 700 °C for 8 h in air and the TiO_2-modified $LiMn_2O_4$ was obtained.

Powder X-ray diffraction (XRD, Rigaku, Rint-2000) using Cu Kα radiation was used to identify the crystalline phase of the TiO_2-modified $LiMn_2O_4$ powders. The particle morphology of TiO_2-modified $LiMn_2O_4$ powders was observed using a scanning electron microscope (SEM, LEO1530), and EDS analysis was used to analyze the element content of the particle surface.

Charge/discharge cycles were carried out in two-electrode cells. The cell consisted of a cathode and a lithium metal anode separated by a cellgard 2003 film. The cathode was fabricated from a mixture of 80 wt% of the $LiMn_2O_4$ powders and 12 wt% of conducting binder (PVDF) and 8 wt% of graphite. The cathode material was cast onto an aluminum foil. The electrolyte used for the electrochemical test is a commercial electrolyte with 1 M $LiPF_6$ dissolved in 1:2 mixture of ethylene carbonate (EC) and dimethyl carbonate (DMC). The charge/discharge cycling was carried out galvanostatically at a current rate of $1C$ (100 mAh g^{-1}) between 3.0 and 4.8 V at room temperature and between 3.0 and 4.25 V at 55 °C respectively.

3. Results and discussion

3.1. Morphology analysis

Fig. 1 shows the SEM images of the pristine $LiMn_2O_4$ powders and the TiO_2-modified $LiMn_2O_4$ powders. The particles of pristine $LiMn_2O_4$ (Fig. 1a) and the TiO_2-modified $LiMn_2O_4$ (Fig. 1b) are both around 1 μm and have perfect shape of spinel. Accordingly, it can be confirmed that the particle shape and size were not changed so much after TiO_2 modification. The particles of the pristine $LiMn_2O_4$ have well-developed (1 0 0) planes and very keen edges (Fig. 1a). For the TiO_2-modified $LiMn_2O_4$ particles, the edges are not as keen as in Fig. 1a and the surface of TiO_2-modified $LiMn_2O_4$ particles (Fig. 1b) is not as steep as the pristine $LiMn_2O_4$ particles (Fig. 1a). So we can say the surface morphology of $LiMn_2O_4$ spinel is changed by TiO_2 modification Fig. 1c shows the EDS spectrum of element content in the region indicated in Fig. 1b and the results were listed in Table 1. Three obvious Ti peaks are observed besides Mn and O in Fig. 1c, which correspond to the Ti content of 0.5% atom in Table 1. This implies that the Ti has been deposited onto the particle surface of $LiMn_2O_4$.

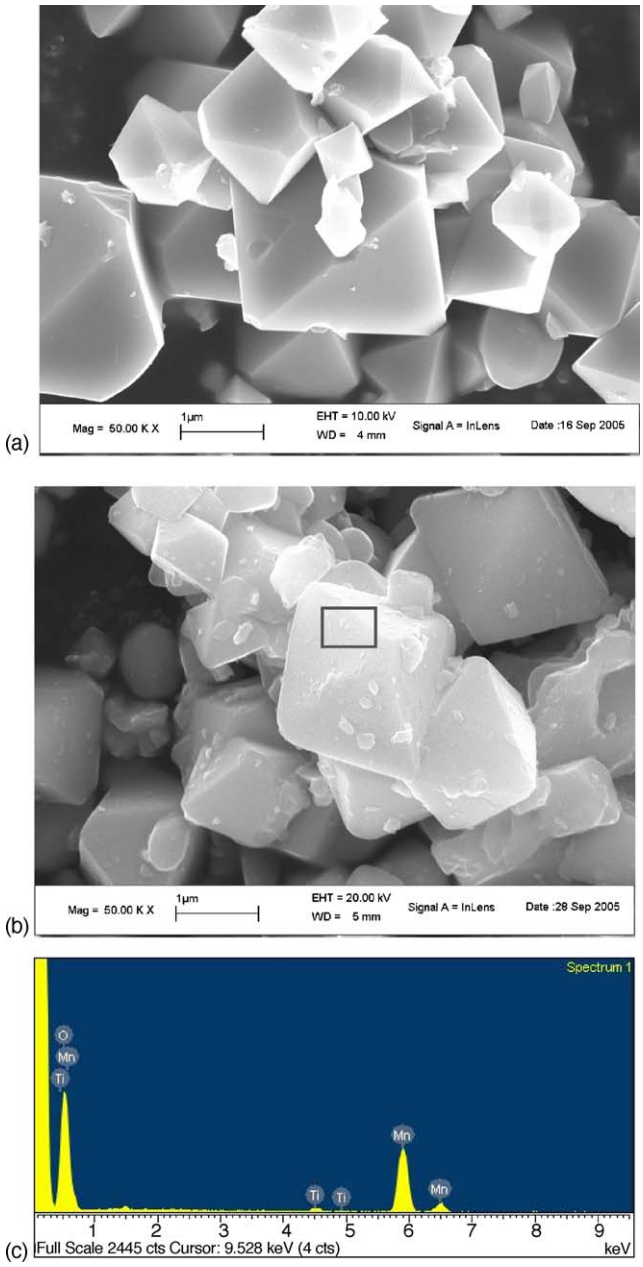

Fig. 1. (a) SEM image of pristine $LiMn_2O_4$ (scale bar: 1 μm), (b) SEM image of TiO_2-modified $LiMn_2O_4$ (scale bar: 1 μm), and (c) EDS spectra of the selective position in (b).

3.2. Structure analysis

Fig. 2 compares the XRD patterns of pristine spinel $LiMn_2O_4$ and the TiO_2-modified $LiMn_2O_4$. The XRD patterns of the samples were indexed as spinel phases. No additional peaks for other phases such as TiO_2, Li_2MnO_3, $LiMnO_2$ or MnO_x can be observed. In addition, peak relative intensities of TiO_2-coated $LiMn_2O_4$ are almost the same as those of pristine $LiMn_2O_4$. This means the normal spinel structure is preserved. However, refinements to the XRD patterns indicate that the lattice parameter of the TiO_2-modified spinel ($a_0 = 8.20774$ Å) is smaller than that of pristine spinel $LiMn_2O_4$ ($a_0 = 8.22113$ Å). According to Hernan et al. [8], Ti can doped into the spinel $LiMn_2O_4$ by replacing Mn and retain the spinel structure. So we may propose that a solid spinel compound of $LiTi_xMn_{2-x}O_4$ was formed on the surface of spinel $LiMn_2O_4$ during heat treatment and caused the shrinkage of the lattice.

Table 1
Element content of the TiO_2-modified $LiMn_2O_4$ obtained from EDS analysis

Element	Weight (%)	Atomic (%)
O	59.61	83.47
Ti	1.08	0.50
Mn	39.31	16.03
Totals	100.00	100.00

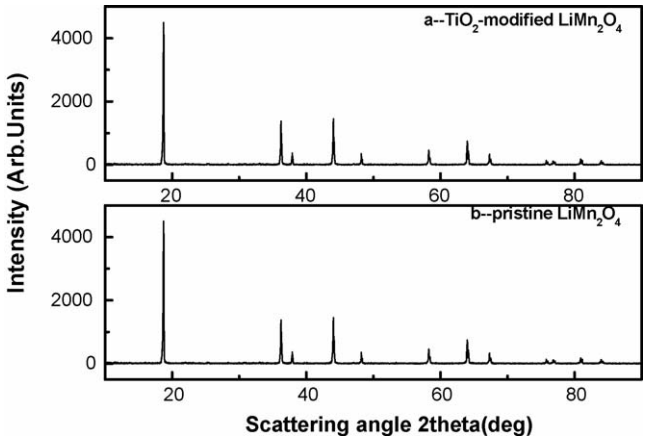

Fig. 2. XRD patterns of: (a) the TiO_2-modified $LiMn_2O_4$ powders and (b) pristine $LiMn_2O_4$ powders.

3.3. Electrochemical properties at high working potential

The pristine $LiMn_2O_4$ powders are commercial material and has a lower initial capacity than that synthesized in laboratory. Fig. 3 a shows the capacity cyclability between 3.0 and 4.8 V of lithium cells using lithium as anode and pristine $LiMn_2O_4$ and TiO_2-modified $LiMn_2O_4$ as cathode, respectively, at room temperature and 1*C* charge–discharge rate. The discharge capacity of pristine $LiMn_2O_4$ shows a fast decline with a capacity loss of 30% of the initial value after only 40 cycles. However, the cyclability of TiO_2-modified $LiMn_2O_4$ is significantly improved, the capacity loss is less than 15% of its initial capacity after 60 cycles. The initial capacity of TiO_2-modified $LiMn_2O_4$ reaches 104 mAh g^{-1} which is much higher than that reported by Hernan et al. [8] (about 80 mAh g^{-1}) who doped Ti into the whole spinel $LiMn_2O_4$ and proposed that Ti^{4+} may increase electrostatic repulsion between the cations occupying (16d) octahedral sites and therefore decrease the capacity and deteriorate the capacity fading during cycling. In contrast, we maintain the inner structure of $LiMn_2O_4$ spinel, only the surface changed by TiO_2 modification, and keep the capacity and reduce the capacity fading. We have also found that the initial capacity of TiO_2-modified $LiMn_2O_4$ is higher than that of pristine $LiMn_2O_4$ both at high working potential and at elevated temperature of 55 °C, as is shown in Fig. 3a (104 mAh g^{-1} versus 96 mAh g^{-1}) and Fig. 5a (103 mAh g^{-1} versus 101 mAh g^{-1}). We want to attribute this to the rapid Li^+ diffusion caused by the $LiTi_xMn_{2-x}O_4$ which may reduce the polarization during cycling, which can be supported by the impedance measurement results in Fig. 4. Fig. 4 shows the electrochemical impedance spectroscopy (EIS) for the pristine $LiMn_2O_4$ and the TiO_2 modified $LiMn_2O_4$. It can be seen that the cell resistance shifts from 1.07 to 0.67 Ω after modification, and the loop diameter shifts from 0.89 to 0.43 Ω, being reduced more than the half. This implies the Li ion diffusion is enhanced in the TiO_2 modified $LiMn_2O_4$ more than in the pristine modified $LiMn_2O_4$. In addition, the electronic resistance is also reduced from 0.24 to 0.18 Ω which means the whole cell electronic conductivity is increased by TiO_2 modification.

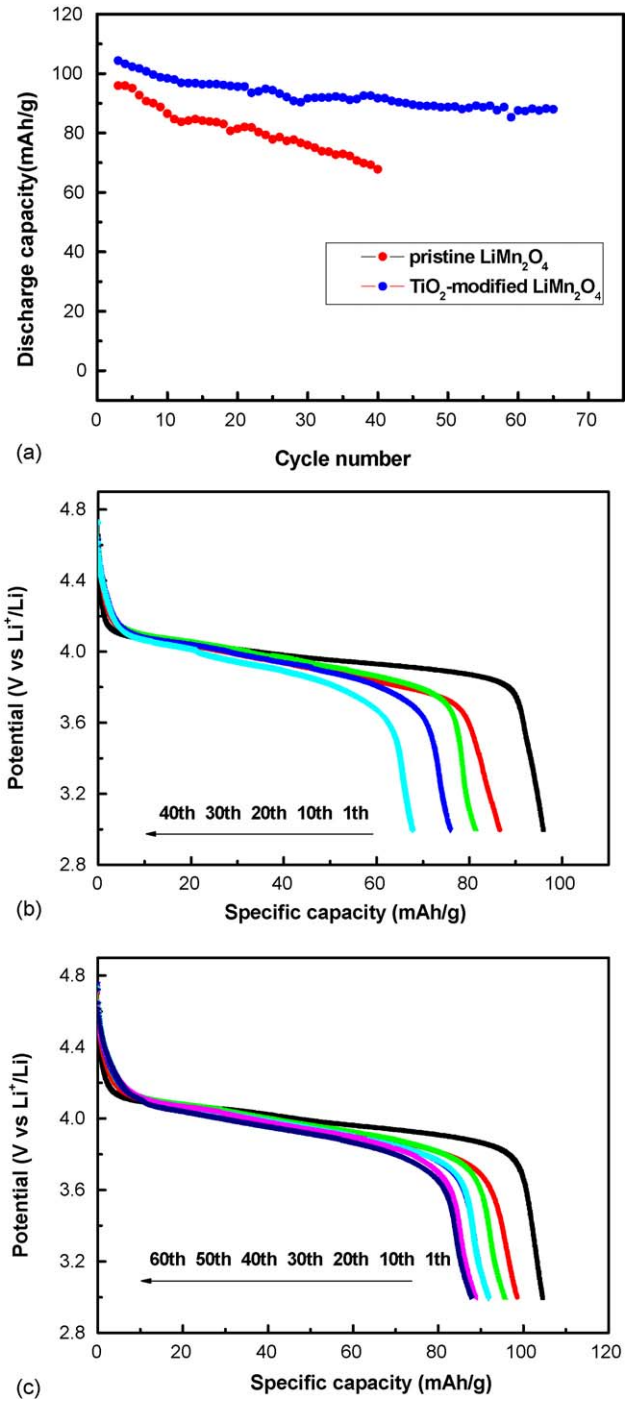

Fig. 3. Cycling behaviors of the samples between 3.0 and 4.8 V at room temperature. (a) Comparison of cyclability of TiO_2-modified $LiMn_2O_4$ with pristine $LiMn_2O_4$ at 1*C*, (b) the first 40 cycles of the pristine $LiMn_2O_4$ at 1*C*, and (c) the first 60 cycles of the TiO_2-modified $LiMn_2O_4$ at 1*C*.

Fig. 3 b and c show the discharge profiles of pristine $LiMn_2O_4$ and TiO_2-modified $LiMn_2O_4$ at 1*C* charge/discharge rate in the potential range of 3.0–4.8 V. Two plateaus of above and below 4.0 V can be recognized obviously in the discharge curves during the first several cycles. However, the cyclability of the pristine $LiMn_2O_4$ deteriorates seriously and the two potential plateaus are shortened rapidly, which causes the capacity fade

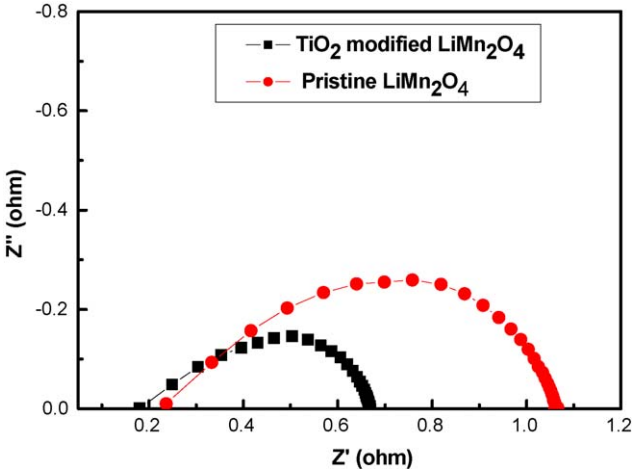

Fig. 4. Electrochemical impedance spectroscopy (EIS) of the cell for the pristine $LiMn_2O_4$ cathode and TiO_2-modified $LiMn_2O_4$ cathode with testing frequency from 100 kHz to 0.01 Hz at room temperature.

quickly. In the contrary, the two plateaus in discharge curves of TiO_2-modified $LiMn_2O_4$ are shaped well and can be obviously recognized after 60 cycles. This may be due to the stable spinel structure caused by the surface layer $LiTi_xMn_{2-x}O_4$ at a high working potential during charge/discharge.

3.4. Electrochemical properties at high temperature condition

Spinel $LiMn_2O_4$ was believed to be the most promising cathode materials of lithium-ion batteries due to its low cost and nontoxicity. However, its poor electrochemical cyclability at elevated temperature hindered its application in commercial lithium-ion batteries [17]. Fig. 5a shows the capacity cyclability of pristine $LiMn_2O_4$ and TiO_2-modified $LiMn_2O_4$ at 1*C* charge–discharge rate between 3.0 and 4.25 V at 55 °C. It is clear that surface modification significantly improves the cyclability of $LiMn_2O_4$ at elevated temperature of 55 °C. Both samples show nearly the same discharge capacity of more than 100 mAh g^{-1}, actually the TiO_2-modified $LiMn_2O_4$ shows higher initial capacity than the pristine $LiMn_2O_4$. The capacity retention of the TiO_2-modified $LiMn_2O_4$ is near to 90% of the initial capacity after 30 cycles, demonstrating the extraordinary cycling stability at elevated temperature, while the pristine $LiMn_2O_4$ electrode suffered a more than 70% capacity loss after 25 cycles.

Fig. 5b and c shows the discharge profiles of pristine $LiMn_2O_4$ and TiO_2-modified $LiMn_2O_4$ at 1*C* charge/discharge rate between 3.0 and 4.25 V. Two plateaus at 3.94 and 4.11 V can be recognized obviously in the discharge curves during the first several cycles. However, the separated plateaus cannot be found after 10 cycles in pristine $LiMn_2O_4$.

It is well known that structural transformation of spinel $Li_xMn_2O_4$ occurs during Li^+ intercalation and deintercalation. Yang et al. [18] gave experimental evidences of the three-phase model of phase transitions in $Li_xMn_2O_4$ cathode materials. These phase compositions are proposed to be $Li_{0.25}Mn_2O_4$, $Li_{2/3}Mn_2O_4$, and $LiMn_2O_4$ [19], corresponding to the potential inflection points at 4.25, 4.10 and 3.91 V versus Li/Li^+ respectively, which were also found to exhibit different superlattices [20,21]. In our experiment, we observe the potential inflections at 4.2, 4.1 and 3.9 V versus Li/Li^+ in the discharge curves. These are consistent with the above results. From Fig. 5b and c, we can see both the initial discharge curves of pristine

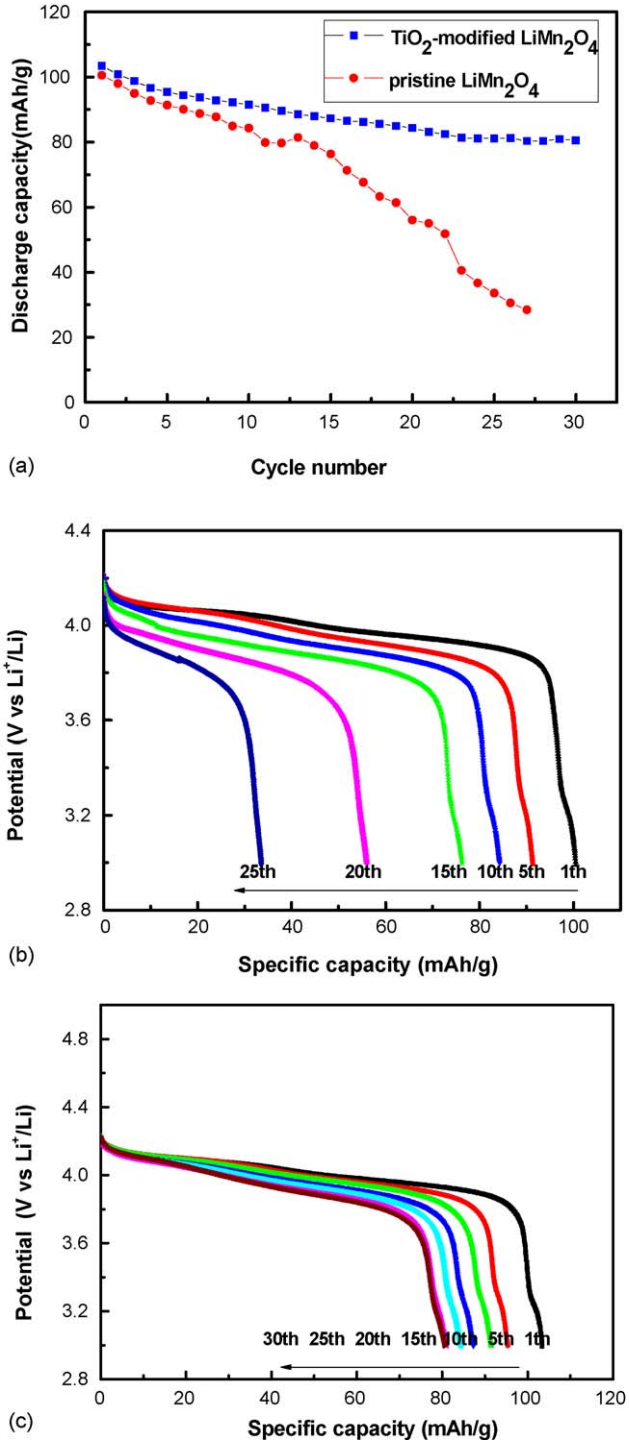

Fig. 5. Cycling behaviors of the samples between 3.0 and 4.25 V at 55 °C. (a) Comparison of cyclability of TiO_2-modified $LiMn_2O_4$ with pristine $LiMn_2O_4$ at 1*C*, (b) the first 25 cycles of the pristine $LiMn_2O_4$ at 1*C*, and (c) the first 30 cycles of the TiO_2-modified $LiMn_2O_4$ at 1*C*.

$LiMn_2O_4$ and TiO_2-modified $LiMn_2O_4$ give two well-shaped plateaus. However, the cyclability of the pristine $LiMn_2O_4$ deteriorates seriously and the first potential plateau disappears after 10 cycles and the second plateau also leans rapidly, which causes the capacity fade quickly. In the contrary, the two plateaus in discharge curves of TiO_2-modified $LiMn_2O_4$ are shaped well and can be obviously recognized after 30 cycles. We can attribute this distinction to the difference of the structure stability and Li^+ conductivity between pristine $LiMn_2O_4$ and TiO_2-modified $LiMn_2O_4$ during charge/discharge. In the pristine $LiMn_2O_4$, the relatively slower Li^+ transfer compared to the electronic reaction rate causes the distortion of the phases discussed above and the disordering of Li^+, resulting in bad cyclability at elevated temperature. However, in the TiO_2-modified $LiMn_2O_4$, the surface layer $LiTi_xMn_{2-x}O_4$ with a expedite Li^+ insertion and extraction can keep the spinel structure stable which consequently presents a better electrochemical performance. Furthermore, the formation of solid layer $LiTi_xMn_{2-x}O_4$ changes the surface proprieties of the spinel $LiMn_2O_4$ and might partly suppress the dissolution of the Mn ions from the spinel into the electrolyte and the corresponding phase transitions, which can also improve the electrochemical performance of $LiMn_2O_4$.

3.5. Differential of the capacity curves

In order to better understand the performance of TiO_2-modified $LiMn_2O_4$ at high-temperature and high potential, we compared the differential capacity curves which were obtained by differential analysis of the discharge curves in Figs. 3 and 5. Fig. 6 shows the differential curves of cells cycled at 55 °C with the charge/discharge rate of 1*C*. Two peaks can be observed corresponding to the two plateaus in the discharge curves in Fig. 5b and c. In Fig. 6a (pristine $LiMn_2O_4$), the '1th' curve has the first peak potential of 4.06 V with the peak intensity of 516 mAh g^{-1} V^{-1} and the second peak potential of 3.95 V with the peak intensity of 485 mAh g^{-1} V^{-1}. However, with the further cycling both peaks shift to lower potential and the peak intensity decreases rapidly. Especially the first peak decreases more quickly than the second peak, and after 25 cycles the first peak disappears. In contrast to Fig. 6a, the curves in Fig. 6b (TiO_2-modified $LiMn_2O_4$) have better performances. The '1th' curve has the first peak potential of 4.09 V with the peak intensity of 561 mAh g^{-1} V^{-1} and the second peak potential of 3.98 V with the peak intensity of 476 mAh g^{-1} V^{-1}. The first peak potential has even unnoticeable changes and both of the two-peak intensities decrease obviously slower than those of pristine

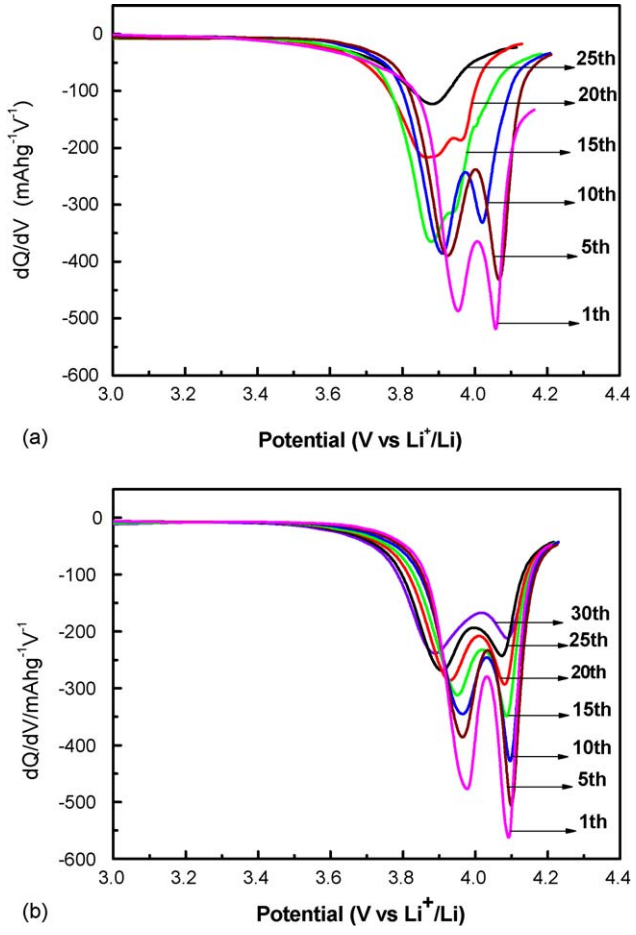

Fig. 6. Differential discharge capacity–voltage relationship after different cycles between 3.0 and 4.25 V at 55 °C of: (a) the pristine $LiMn_2O_4$ at 1*C*, (b) the TiO_2-modified $LiMn_2O_4$ at 1*C*.

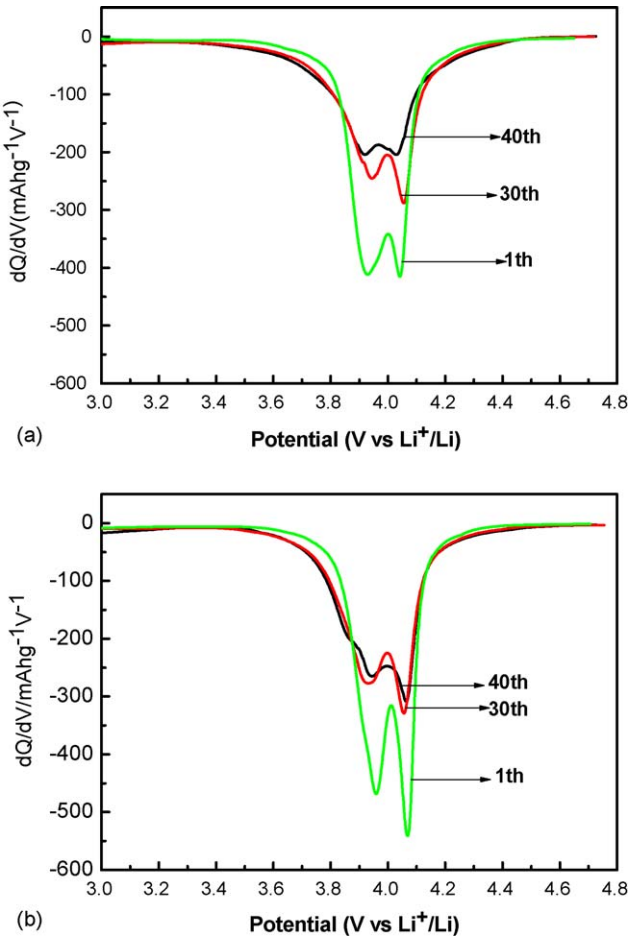

Fig. 7. Differential discharge capacity–voltage relationship after different cycles between 3.0 and 4.8 V at room temperature of: (a) the pristine $LiMn_2O_4$ at 1*C*, (b) the TiO_2-modified $LiMn_2O_4$ at 1*C*.

$LiMn_2O_4$ during the cycling. After 30 cycles the discharge curve still has the first peak intensity of 210 mAh g^{-1} V^{-1} and the second peak intensity of 236 mAh g^{-1} V^{-1}.

Fig. 7 shows the differential capacity curves of the pristine $LiMn_2O_4$ and the TiO_2-coated $LiMn_2O_4$ after different cycles between 3.0 and 4.8 V at room temperature at 1*C*. In Fig. 7a the '1th' curve has the first peak potential of 4.04 V with the peak intensity of 413 mAh g^{-1} V^{-1} and the second peak potential of 3.92 V with the peak intensity of 410 mAh g^{-1} V^{-1}. While in Fig. 7b, the '1th' curve has the first peak potential of 4.07 V with the peak intensity of 540 mAh g^{-1} V^{-1} and the second peak potential of 3.95 V with the peak intensity of 466 mAh g^{-1} V^{-1}. After 40 cycles the curve still has the higher peak potential and peak intensity in Fig. 7b than that in Fig. 7a. Furthermore, the two peaks are separated better in Fig. 7b than in Fig. 7a.

From Figs. 6 and 7, we can see the discharge peak potential and the peak intensity are both enhanced by TiO_2 modifying compared to the pristine $LiMn_2O_4$. The result is consistent with the discussion in Figs. 3 and 5. Most importantly, the first peak intensity at the elevated temperature of 55 °C is improved most obviously among all the improved properties by the sol–gel method of TiO_2 modifying. Differently said, the electrochemical performance of $LiMn_2O_4$ is improved more obviously at elevated temperature than at high working potential by TiO_2 modification.

4. Conclusions

The surface of spinel $LiMn_2O_4$ was modified by TiO_2 and a layer of $LiTi_xMn_{2-x}O_4$ was formed on the surface of $LiMn_2O_4$ particles. TiO_2-modified $LiMn_2O_4$ shows excellent electrochemical properties after high potential and elevated-temperature cycling by improving Li^+ conductivity and stabilizing the phase structure. Among the whole improvement of the $LiMn_2O_4$ electrochemical performance at high working potential and at elevated temperature by TiO_2 modifying, the high potential plateau is improved most distinctly. Therefore, surface TiO_2 modifying on $LiMn_2O_4$ is a very promising treatment of $LiMn_2O_4$ for lithium-ion batteries.

Acknowledgement

This work was financially supported by the State Key Basic Research Program of China (2002CB211803).

References

[1] J.M. Tarascon, E. Wang, F.K. Shokoohi, J. Electrochem. Soc. 138 (1991) 2859.
[2] M.M. Thackeray, P.J. Johnson, L.A. De Picciotto, P.G. Bruce, J.B. Goodenough, Mater. Res. Bull. 19 (1984) 179.
[3] M.M. Thackeray, L.A. Depicciotto, A. de Kock, P.J. Johnson, V.A. Nicholas, K.T. Adendorff, J. Power Sources 21 (1987) 1.
[4] Y. Xia, N. Kumada, M. Yoshio, J. Power Sources 90 (2000) 135.
[5] M.M. Thackeray, Y. Shao-Horn, A.J. Kahaian, K.D. Kepler, E. Skinner, J.T. Vaughey, S.J. Hackney, Electrochem. Solid-State Lett. 1 (1998) 7.
[6] M.M. Thackeray, J. Am. Ceram. Soc. 82 (1999) 3347.
[7] A. Yamada, M. Tanaka, Mater. Res. Bull. 30 (1995) 715.
[8] L. Hernan, J. Morales, L. Sanchez, J. Santos, Solid State Ionics 118 (1999) 179.
[9] S.S. Zhang, Y.R. Jow, J. Power Sources 109 (2002) 172.
[10] J.M. Tarascon, D. Gnyomand, J. Electrochem. Soc. 138 (1991) 2864.
[11] W. Liu, G.C. Farrington, F. Chaput, B. Dunn, J. Electrochem. Soc. 148 (2001) A687.
[12] I. Taniguchi, D. Song, M. Wakihara, J. Power Sources 109 (2002) 333.
[13] G.G. Amatucci, A. Blyr, C. Sigala, P. Alfonse, J.M. Tarascon, Solid State Ionics 104 (1997) 13.
[14] S.F. Yang, W. Luo, Y.C. Zhu, Y.H. Liu, J.Z. Zhao, Z.C. Wang, G.T. Zhou, Chem. J. Chin. Univ. 24 (2003) 1933.
[15] L. Kavan, M. Gräizel, J. Rathousk, A. Zukalb, J. Electrochem. Soc. 143 (1996) 394.
[16] M. Wagemaker, A.A. van Well, G.J. Kearley, F.M. Mulder, Solid State Ionics 175 (2004) 191.
[17] Y. Sun, Z. Wang, L. Chen, X. Huang, J. Electrochem. Soc. 150 (2003) A1294.
[18] X.Q. Yang, X. Sun, S.J. Lee, J. McBreen, S. Mukerjee, M.L. Daroux, X.K. Xing, Electrochem. Solid-State Lett. 2 (1999) 157.
[19] H. Bjork, T. Gustafsson, J.O. Thomas, S. Lidinb, V. Petricek, J. Mater. Chem. 13 (2003) 585.
[20] I.D. Brown, D. Altermatt, Acta Crystallogr. B 41 (1985) 244.
[21] P. Strobel, A. Ibarra-Palos, C. Bougerol, Lithium Battery Discussions—Electrode Materials, Arcachon, France, 2001 (abstract no. 16).